Development of Macro-Micro-Kinematics for Micro-Assembly

Christian Pape, Klaus Haskamp, Alexej Janz
Institute of Measurement and Automatic Control, Leibniz Universität Hannover
Nienburger Str. 17, 30167 Hannover Germany
email: alexej.janz@imr.uni-hannover.de

Abstract
The existing precision robot µ316-KROS at the Institute of Measurement and Automatic Control is intended to be used for micro-assembly. In this paper we will discuss necessary measures. Necessary are an optimized controller, improved control technology and extended path planning. To assure the absolute accuracy of the robot, a calibration is in progress. To increase the resolution of the robot and decrease vibrations at controlled standstill, a piezo actuator is also used.

Keywords:
Robotics, micro-assembly, piezo actuators, control, path planning

1 INTRODUCTION

The enormous potential of miniaturization is varied and goes far beyond the sheer volume and weight reduction. Thus, reduced power consumption and more functions per volume are important benefits of micro-technical solutions. The benefits of this miniaturization are particularly visible in microelectronics. Here, the bit density has averagely doubled every three years. After the assembly of monolithic components, the next step in this development is the assembly of hybrid components. That means that while in the current state of research in micro systems technology it is possible to built micro-electronics, micro-mechanical and micro-optical components individually [1], the assembly of individual components is extremely demanding and has so far only be done in one plane (2D). A central role is played by the micro-assembly, which assembles the individual components on a common carrier or substrate. For a further spread of the micro-hybrid systems, it is necessary to establish a wide variety of actuators, which can produce micro systems in the small to medium series [2].

2 PROJECT GOALS

The aim of this project is the precision control of robots with the help of image feedback and in combination along with additional piezomechanics in the micron range. The Institute of Measurement and Automatic Control is working on the assembly of plastic components hot embossed with application-specific electronics. The existing hot embossing machine HEX 03 can manufacture optical components such as lenses or mechanical parts such as gears. These can then be assembled with micro-electronic components such as customer-specific integrated circuits (ASICs) or programmable logic devices (PLD).

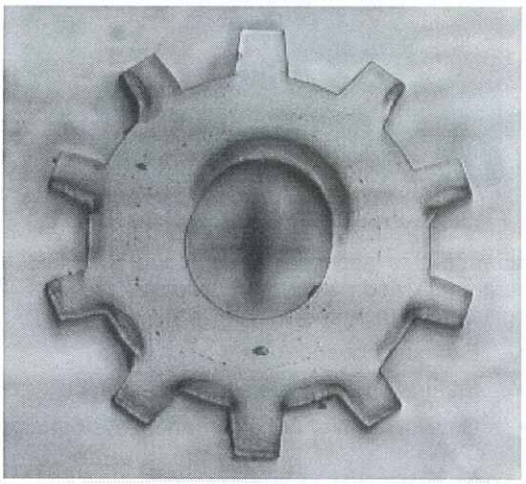

Figure 1: Hot embossed gear (diameter 600 microns), © IMR

3 APPROACH

At the institute two 6-axis precision robots µ316 KROS are available for the assembly. These are especially capable for the assembly of micro systems due to their extremely high repeatability of 5 microns at the end effector. To avoid position deviations due to heat extension the robot was symmetrically designed. Because of this, the torsion caused by heating is largely compensated. In addition, the robot has nine direct drive motors, so that the accuracy is not affected by the tolerance of the gearbox.

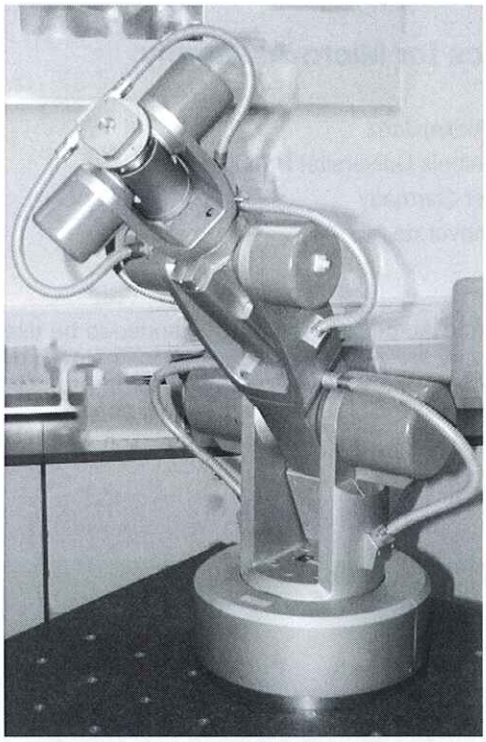

Figure 2: Precision Robot µ316-KROS, © IMR

To increase this accuracy even further the Institute of Measurement and Automatic Control follows three strategies at the moment:

- Exchange of controller
- Integration of a piezoelectric Actuator
- Development of a measurement system

4 ROBOT CONTROL OPTIMIZATION

Although the robot is composed of state of the art components the existing control has a restored development status. Unlike there has been a lower enhancement with the mechanics, the motors and the power electronics in the last years. Therefore an industrial control from the company "Delta-Tau" was integrated in the robot. Some features of this industrial control are:

- Rotary encoder offers a 128-times interpolation, therefore a resolution of 2 million counts per revolution is possible
- Automatic sinus-commutation of the direct current motors
- A simultaneous automatic control up to 32 axes is possible

4.1 Standard-Control-Concept

The standard controller is a time discrete PID controller with a velocity and an acceleration feedforward term. To attain an acceptable quality of control the actuating variable is strained with a notch-filter. The function of the notch-filter is to compensate structural vibrations of the axes, which are caused through the notch detent torques.

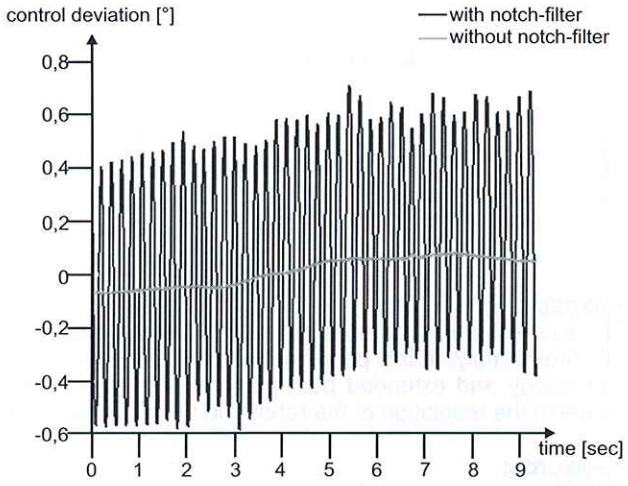

Figure 3: Control deviation with and without notch-filter, © IMR

4.2 Adjusted control concept

The control path from robots can be described with the equations of motion and offers a strong non-linear character. Because of the permanent changes of the control path the quality of the PID-controller is suboptimal in the whole working area.

To enhance the effort in the entire operation range the actual development is to elaborate new control concepts to adapt the controller to the control path. One strategie is constituted by the moment feedforward controller and tries to compensate the nonlinearities in order to disburden the controller.

Another concept is an adaptive controller [3]. In order to minimize the Euclidian control error $\|e\|^2$ the parameters p are adapted to the path:

$$\|e(t)\|_e^2 = \|w(t) - y(t)\|^2$$

with

$$y(t) = f(p, w, t)$$

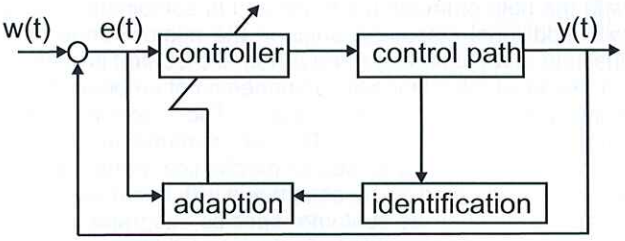

Figure 4: Control strategy, © IMR

This strategy requires a model of the control path, whose parameters can be identified online for example with a kalman-filter or an observer. Both, the information and the control error, constitute the inputs for the adaption.

The model can be described as a multi body system. For the computation of the equations of motion e.g. the principle of conversation of angular momentum concerning the point O in the inertial frame can be used:

$$\frac{{}^{I}d}{dt}\vec{L}^{O} = \vec{M}^{O}_{external}$$

with $\frac{{}^{I}d}{dt}\vec{L}^{O}$ as the time derivation of spin and $\vec{M}^{O}_{external}$ as the amount of the external moments.

Another way to calculate the differential equations is to use the Lagrange formalism:

$$M_i = \frac{d}{dt}\frac{\delta L}{\delta \dot{\mathbf{q}}_i} - \frac{\delta L}{\delta \mathbf{q}_i}$$

with

$$L = K - P = \sum_{j=1}^{n} K_j(\mathbf{q}, \dot{\mathbf{q}}) - \sum_{j=1}^{n} P_j(\mathbf{q})$$

L describes the Lagrange-function, M_i the sum of the external moments and $\mathbf{q}$ the generalized coordinates, normally the joint angles. Furthermore K_j and P_j are the kinetic and the potential energy of the body with the index j.

In favour of programming and testing several identification methods it is important to implement the model in the simulation environment "simulink" of the software "matlab".

5 PATH PLANING

The controller from the company „delta-tau" just offers the ability to move the axes in their own coordinate systems. Because of this a Cartesian positioning of the endeffektor cannot be achieved as easy as an angularity approach of the axes.

To accomplish a given position and orientation a method for a numerical calculation of the inverse kinematic based on a nonlinear optimization was developed [4]. With the aid of the forward kinematics $\mathbf{f}(\mathbf{q})$, developed with the denavit-hartenberg-notation, a functional ε can be established, whose minimum constitutes the result of the inverse kinematics [4, 5]:

$$\varepsilon = \|\Delta \mathbf{x}\|$$

$$\Delta \mathbf{x} = \mathbf{x}_{given} - \mathbf{f}(\mathbf{q})$$

$\Delta \mathbf{x}$ ist the difference vector between the given position $\mathbf{x}_{given}$ and the forward kinematic $\mathbf{f}(\mathbf{q})$ to a specified joint angularity $\mathbf{q}$.

The joint angularity $\mathbf{q}^*$, for which the functional ε achieves a value near zero, is the result of the inverse kinematic [4].

The minimum $\mathbf{q}^*$ can be located with the "rosenbrock-procedure". The "rosenbrock-procedure" is a method for finding a minimum or a maximum of a function. The advantage is, that the algorithm works without the use of the gradient. To begin a nonlinear optimization-algorithm a start vector $\mathbf{q}_{start}$ and an initial value $\varepsilon(\mathbf{q}_{start})$ of the functional ε is required. The schedule of the used "rosenbrock-procedure" is shown in figure 5.

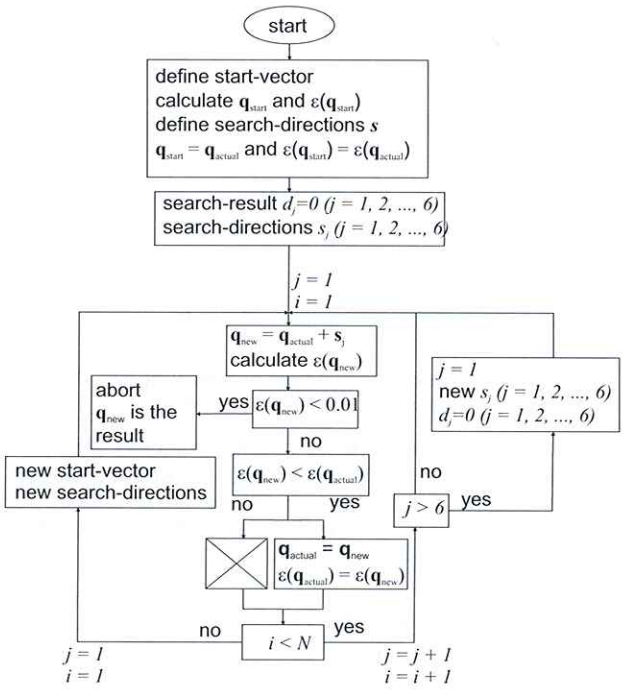

Figure 5: Schedule of the modified „rosenbrock-algorithm", © IMR

The algorithm was coded in „C++". Additionally the algorithm was modified and it will restart the minimum search, if no result was found after "N" steps. This behavior occurs in consequence of a badly chosen start vector $\mathbf{q}_{start}$. To avoid the problem that the algorithm always finds the same local minimum, a new start vector, based on random-values, is created whenever the algorithm restarts.

All numeric optimization methods are approximation methods. In fact of that a break condition for the finding of the minimum must be formulated. In this case, $\mathbf{q}^*$ is a result, if the fault between the given and the calculated position ε is lower than 0.01. Out of it a maximum position fault of 100 µm respectively a maximum orientation fault of 100 µ° remains at the end of the calculation. If a more accurate positioning of the endeffector is required a smaller value for the error boundary can be chosen. Thereby the difference between the given and the calculated pose will be smaller at the end of the computation.

To show the robustness and the quality of the algorithm the inverse kinematics for a given pose $\mathbf{x}_{given}$ was calculated with the modified "rosenbrock-procedure". Figure 6 illustrates the development of the magnitude of the functional ε. The figure points out that the fault between the given pose and the forward kinematic is already after 30 iterations below the defined boundary of 0.01.

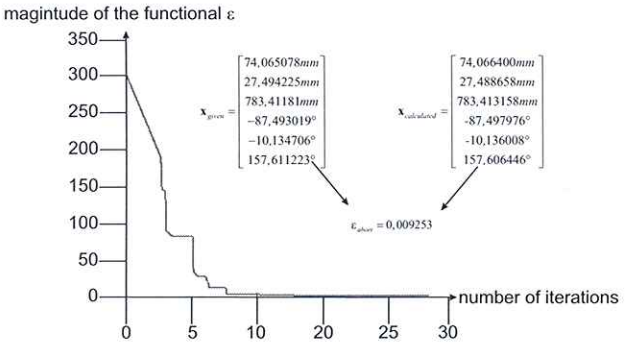

Figure 6: Development of the functioal during the optimization process, © IMR

Constitutive on these results a path planning algorithm based on the computer language „C++" was developed. With the algorithm it is possible to move the endeffector between two points in the 3-dimensional environment along defined paths like lines or circles.

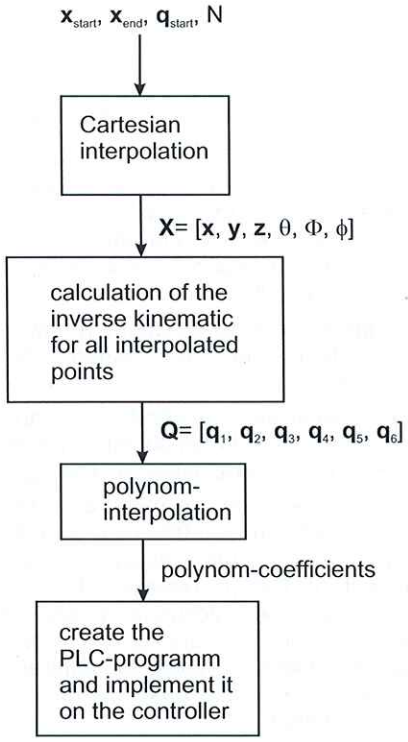

Figure 7: Schedule of the path planing algorithm, © IMR

For the calculation of a linear path a start point $\mathbf{x}_{start}$, an end point $\mathbf{x}_{end}$ and a start vector $\mathbf{q}_{start}$ for the joint angles must be set. $\mathbf{x}_{start}$ and $\mathbf{x}_{end}$ are 6-dimensional vectors and describe the position and the orientation of the endeffector at the beginning and at the end of the move.

In the first step of the algorithm a Cartesian interpolation for each component of the position and the orientation was accomplished and a $N \times 6$ matrix $\mathbf{X}$ was returned, whose lines constitutes the poses along the move. The number N for the interpolation is variable and affects the quality of the generated linear move.

The algorithm calculates the inverse kinematic for all these poses. Many poses are singular and hence the given pose can be reached with different joint angle combinations.

Therefore in the joint angle curve may appear the problem, that there are steps between two consecutive joint positions. To solve this problem, the result $\mathbf{q}_i$ of the calculation of the inverse kinematic from pose i is the start vector $\mathbf{q}_{start,i+1}$ for the calculation of pose $i+1$. Therewith the algorithm may find a result for pose $i+1$, which is near to the joint angles from pose i.

Figure 8 shows the calculated angles of joint 3, whereas the start- and the endpoint were chosen as:

$$\mathbf{x}_{start} = \begin{bmatrix} -306{,}4972mm \\ -154{,}0513mm \\ 777{,}7685mm \\ -66{,}7695° \\ -42{,}8242° \\ 109{,}4828° \end{bmatrix}$$

$$\mathbf{x}_{end} = \begin{bmatrix} 111{,}2432mm \\ 361{,}4866mm \\ 742{,}3944mm \\ -81{,}4539° \\ -11{,}7113° \\ -31{,}1217° \end{bmatrix}$$

The figure demonstrates a consistent angle development.

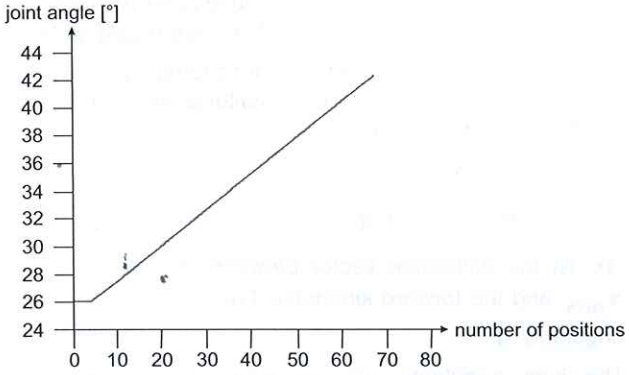

Figure 8: Calculated angle-development of axis 3, © IMR

The memory capacity from the controller "delta-tau" is to small for saving all angles. Thus the target positions were implemented on the controller with polynomials. The functions embody the target positions and were written in a "PLC-program" (**P**rogrammable-**L**ogic-**C**ontroller). The memory capacity of the "PLC-program" is very small and in fact of that it can be implemented on the controller. After activating the program the target-position was calculated for each axis.

Figure 9 shows the composition between the calculated and the real move from axis 3. For the path planning the start- and the endpoint from above was used. The difference between the curves can be explained with the PID-controller. The position of the axis and the gravitation moment increases continuous. For an optimal axis-control the actuating variable must be enhanced to compensate the nonlinear moment.

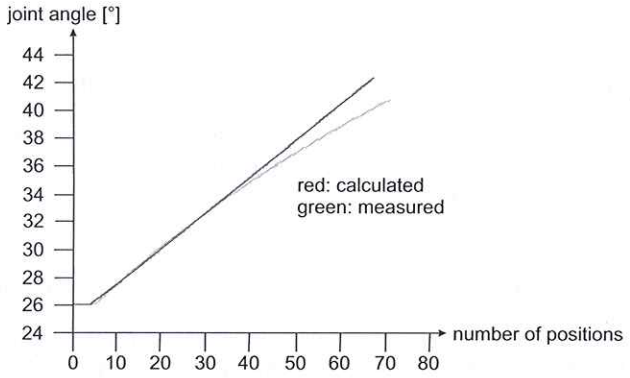

Figure 9: Composition between calculated and real move, © IMR

6 PIEZO ACTUATORS

To offset the limited travel of piezoelectric actuators, the actuator is connected with the precision robot µ316 KROS- to take advantage of the robot (large work space) and the piezo actuator (high accuracy). For that purpose a higher level controller is designed, which supervises the robot and the xyz-table controls.

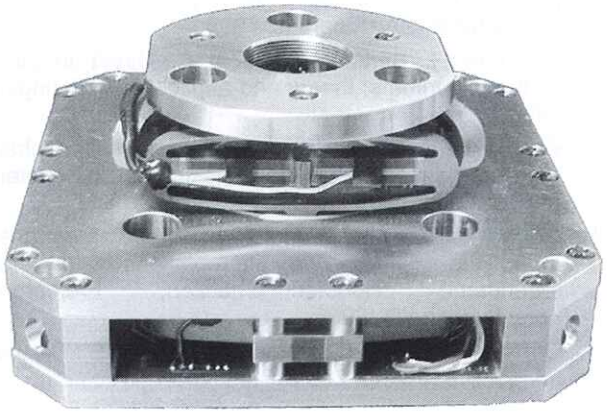

Figure 10: xyz-table with piezoelectric actuators, © IMR

To ensure that the vibration amplitude of the end effector (Tool Center Point) is not bigger than the working area of the piezo actuator, the maximum vibration amplitude of the TCP's is measured. The end effector was placed into work area and then held in controlled standstill. Through measurement of the 6 axis angles and the ideal kinematic smodel, the position of the robot can be reconstructed. Figure 11 shows the movement of the TCP from the desired position in x direction. From the figure it can be taken that a maximum amplitude of 5 microns existed during the controlled standstill.

Since the calculation of the vibration with the ideal kinematic model has been implemented, the measurement of the vibration with a laser Doppler vibrometer (LDV) will serve as a reference. The LDV measures using the so-called Doppler effect. Thereby the target is illuminated with a laser and the frequency of the returning light changes due to the movement of the target. With the Portable Digital Vibrometer PSV-400 from Polytec, the speed of oscillation in the range 0.05 Hz - 22 kHz is recorded with an error of ± 0.2%. To get a distance signal the velocity signal was then numerically integrated (see figure 12). The so-measured vibration amplitude is 2 microns and is a little lower than what was calculated using the forward kinematics, which is probably a consequence of the limited frequency range, the numerical integration and the vibrations of the LDV. The aim is to validate this measurement by using other measuring instruments for example a three-beam interferometer.

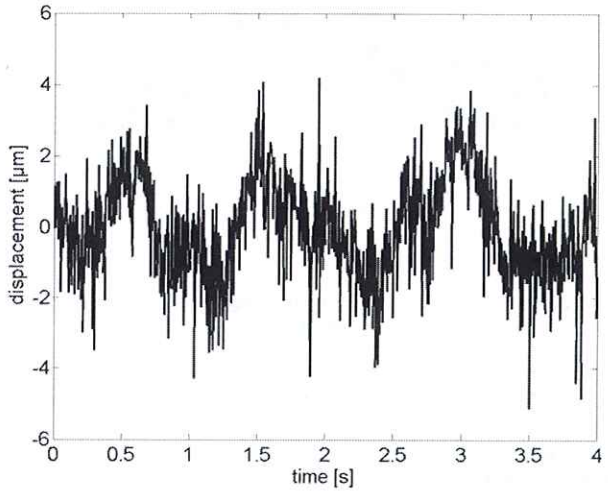

Figure 11: Vibration of the TCPs in x direction calculated using forward kinematics, © IMR

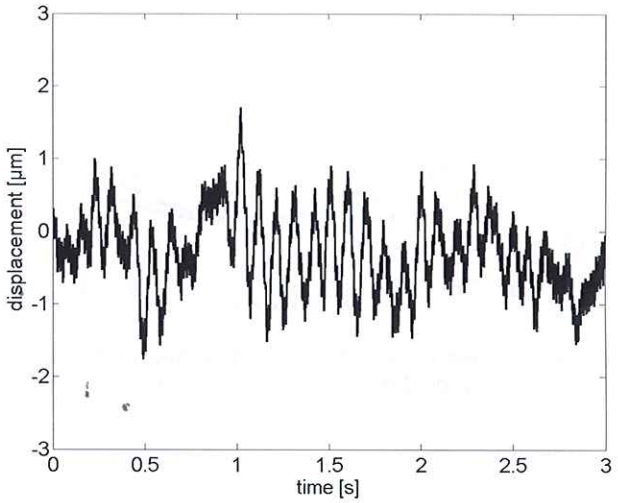

Figure 12: The vibration of the TCP in one direction measured with the LDV, © IMR

7 EXTERNAL MEASUREMENT SYSTEM

In order to compensate the vibration of the robot end effector with help of the piezoelectric actuator, it is necessary to employ an external measurement system, that must estimate the 6D-position (3 coordinates and 3 orientation angles) in real-time.

For this task two high speed CMOS cameras with telecentric lenses measure the position of three white balls on black background. These balls are then mounted on the robot's endeffector.

To test of the measurement system the camera MC1300 with a telecentric lens has been used. This camera makes 123 frames per second and has a field of view of approximately 40x30 mm^2 by a resolution of 800x600 pixels. In this case the optical resolution is approximately 50 µm. With the image processing the sub pixel resolution of 0.05 pixels or 2 µm can be reached [6].

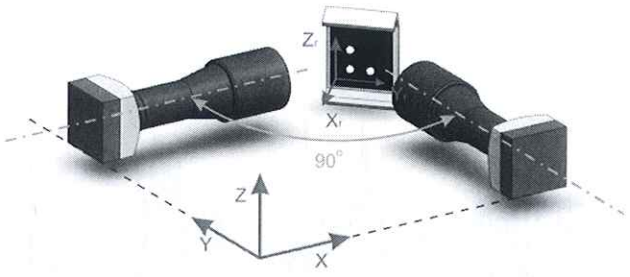

Figure 13: The principle of the measurement system, © IMR

Because the telecentric lenses have depth of ±11 mm, the accuracy of the measurement system depends on the distance between the lens and the mark. This dependence is presented in figure 14. The position of the mark, where the picture is most clear, is *X=0*. It is obvious, that the closer the mark gets to null-position, the higher is the measurement accuracy of the system.

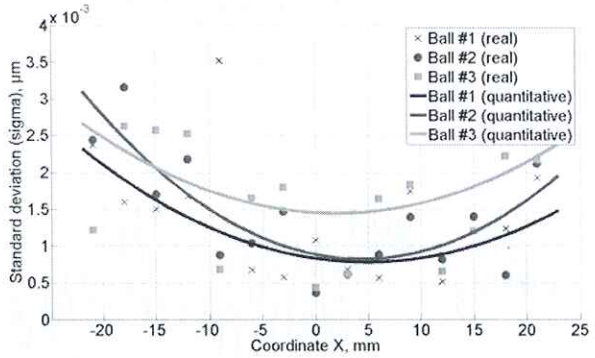

Figure 14: Dependence of the standard deviation from the distance between the lens and the mark with white balls, © IMR

Thereby two cameras with telecentric lenses can be used to measure the 6D-position of the robot's end effector in 3D-space within volume of 40x40x30 mm. The standard deviation of the measured position is 2 µm then. If the distance between the balls on the mark is 10 mm, then the angle deviation is 0.01º.

8 SUMMARY

In the present paper the field of application of the robot was briefly described and some measures to improve the control and regulation were shown. Furthermore, approaches and initial results in the development of a path planning module were presented. To estimate how much the end-effector vibrates, the vibration of the TCP was measured. Also the camera measurement system was implemented to identify the position of the robot with an accuracy of 2 µm.

9 REFERENCES

[1] Reinhart, G.; Höhn, M.: Mikrointegration erfordert neue Montagetechnologien. VDI/VDE-Magazin Technik in Bayern (1999) 3, S. 10 – 11

[2] Westkämper, E., Schünemann, M.; Schlenker, D. u.a.: Produktionskonzepte für die Mikrotechnik in Produktionstechnik für Mikrosysteme. Stuttgart: Frauenhofer IPA-Kongress, 1998

[3] Kaufman, H.; Barkana, I., Sobel, K.: Direct adaptive control algorithms: theory and applications, Springer, 1998

[4] van de Logt, Guido: Entwicklung von numerischen Verfahren zur Planung von Trajektorien für Roboter, Shaker Verlag, 1999

[5] Nawaz, Rashid: Modulares Koordinatentrans-formations- und Bahninterpolationsmodul für redundante Roboterkinematiken, Freiberger Forschungshefte, 2005

[6] Gonsalez Rafael C., Woods Richard E.: Digital Image Processing, 2nd Edition, 2002